

RSC Publishing Faraday Discussions

Probing Ion Current in Solid-Electrolytes at the Meso- and Nanoscale

Journal:	<i>Faraday Discussions</i>
Manuscript ID	FD-ART-03-2018-000071.R1
Article Type:	Paper
Date Submitted by the Author:	21-Apr-2018
Complete List of Authors:	Martinez, Joseph; University of California, School of Physical Sciences Ashby, David; University of California, Los Angeles, Materials Science and Engineering Zhu, Cheng; Indiana University, Department of Chemistry Dunn, Bruce; University of California, Dept of Materials Sci and Eng Baker, Lane; Indiana University, Department of Chemistry; Siwy, Zuzanna; University of California, School of Physical Sciences

SCHOLARONE™
Manuscripts

Probing Ion Current in Solid-Electrolytes at the Meso- and Nanoscale

Joseph Martinez,^a David Ashby,^b Cheng Zhu,^c Bruce Dunn,^b Lane A. Baker,^c Zuzanna S. Siwy^{a,d,e}

Received 00th January 20xx,
Accepted 00th January 20xx

DOI: 10.1039/x0xx00000x

www.rsc.org/

We present experimental approaches to probe ionic conductivity of solid electrolytes at meso- and nanoscales. Silica ionogel based electrolytes have emerged as an important class of solid electrolytes because they maintain both fluidic and high conductivity states at the nanoscale, but at the macroscale they are basically solid. Single mesopores in polymer films are shown to serve as templates for cast ionogels. Ionic conductivity of the ionogels was probed by two experimental approaches. In the first approach, the single-pore/ionogel membranes were placed between two chambers of a conductivity cell, in a set-up similar to that used for investigating liquid electrolytes. The second approach involved depositing contacts directly onto the membrane and measuring conductivity without bulk solution present. Ionic conductivity determined by the two methods was in excellent agreement with macroscopic measurements, which suggested that electrochemical properties of ionogel based electrolytes are preserved at the mesoscale, and ionogels can be useful in designing meso-scaled energy-storage devices.

Introduction

Ionic transport at the nanoscale has been at the center of interest of researchers from different fields. Passage of ions through biological channels is the basis of many physiological processes of living organisms.¹ Moreover, ion transport through nanoscale structures exhibits properties not observed on the microscale.² Cation/anion selectivity,³ rectification of ionic current^{4-5,6,7,8,9,10,11} or water flow,^{12,13} sensitivity to the presence of individual molecules^{14-15,16,17,18} are only a few examples of phenomena characteristic of nanosized channels and pores.

The majority of research on ionic transport at the nanoscale has focused on aqueous solutions due to the relevance of biological channels and applicability to building sensors. Examples of studies in non-aqueous solutions are scarce and include experiments in ionic liquids,^{19,20} organic electrolytes,²¹ and organic solvents.²² Ionic transport in non-aqueous solutions at the nanoscale has been under-explored, even though the topic is important for a variety of applications including separations and energy storage.^{23,24} For the latter family of applications, alternative electrolytes including gel-based electrolytes^{25-26,27} and solid-state electrolytes²⁸ have emerged as interesting options. Our lab has recently performed a series of experiments aimed at measuring ion current through nanopores filled with a PMMA gel containing LiClO₄ in

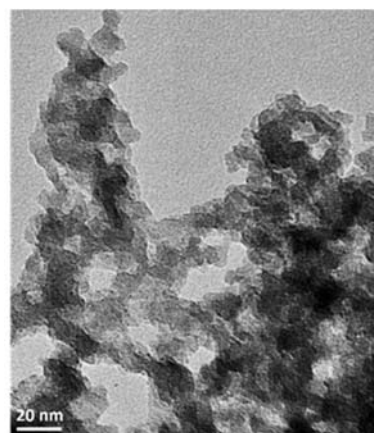


Figure 1. Transmission electron micrograph of an ionogel. (Ionic liquid removed through super critical drying.)

propylene carbonate;^{29,30} the same system was shown before to render an unusual cycle stability of lithium battery.²⁷ Ionic transport of the nanopore/PMMA system was found dependent on the pore shape such that conically shaped gel structures rectified the current, creating a basis for solid ionic diodes.²⁹ PMMA gel used in the experiments was however soft and amenable to swelling in the presence of liquid electrolyte.

In this manuscript we examine ion transport properties of a solid-state electrolyte based on silica ionogel.³² Ionogel electrolytes consist of ionic liquid trapped in a rigid nanoporous support. Ionogels feature much higher conductivity than conventional solid-state electrolytes (e.g., lithium phosphorous oxynitride (LiPON)³¹), because even though they are basically solid at the macroscale, they maintain fluidic/high conductance state at the nanoscale. Ionogels create an attractive alternative to more 'classical' solid electrolytes, also because their synthesis can be adjusted to allow photo-patterning.³²

^a Department of Physics and Astronomy, University of California, Irvine, CA 92697, USA

^b Department of Materials Science and Engineering, University of California, Los Angeles, CA 90095, USA

^c Department of Chemistry, Indiana University, Bloomington, IN 47405-7102, USA

^d Department of Chemistry, University of California, Irvine, CA 92697, USA

^e Department of Bioengineering, University of California, Irvine, CA 92697, USA

E-mail: zsiwy@uci.edu

Tel: +1 (949) 824-8290

Electronic Supplementary Information (ESI) available: [details of any supplementary information available should be included here]. See DOI: 10.1039/x0xx00000x

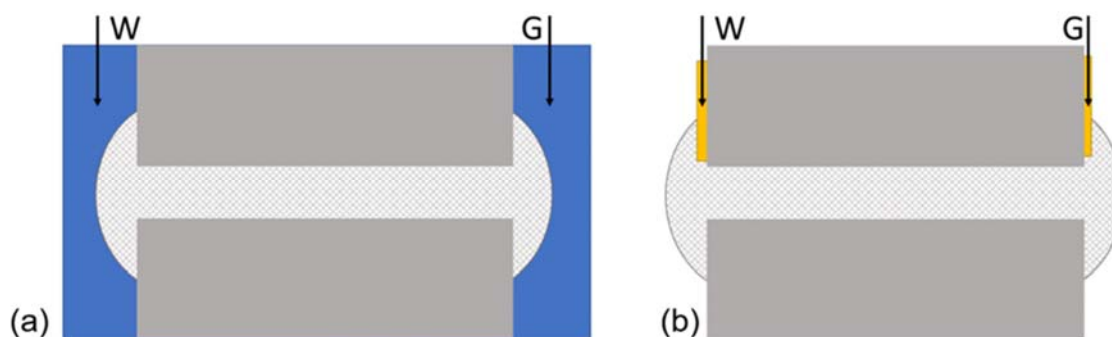


Figure 2. Two experimental approaches used to measure ionic conductivity of a confined ionogel. (a) A single pore filled with the ionogel was placed in contact with an ionic liquid with lithium salt; two electrodes were placed in the liquid; the PET membrane is shown in grey, ionic liquid with lithium in blue, and the patterned region represents the ionogel. (b) A single pore before drop-casting of the ionogel, was sputtered on both sides with 20 nm of Au, which served as the electrical contact ionogel.

Properties of ionogels are typically examined as macroscopic films with a lithium electrode, and lithium containing ionic liquid in an electrochemical cell (e.g., $\text{LiFePO}_4/\text{ionogel}/\text{Li}$), to measure system energy and power densities.

Here we report ionic conductivity of ionogels at the meso and nanoscales probed by measuring ion current carried by all cations and anions present in a solution. Experiments were performed with single polymer pores of tuned geometry filled with the ionogel by drop casting. The ionogel we investigated contained 1-butyl-3-methylimidazolium bis(trifluoromethanesulfonyl) imide (BMIM TFSI) with 500 mM Bis(trifluoromethane) sulfonimide lithium salt (Li TFSI). We also used scanning ion conductance microscopy (SICM) to probe the effective surface charge of the ionogel. Polarity and presence of the effective surface charge is important for interpretation of ionic current measurements and determination of majority charge carriers. To the best of our knowledge, measurements of ionic conductivity of silica ionogels on meso and nanoscales have not been yet performed. Thus this is an exploratory study to demonstrate whether ionic conductivity in silica ionogels is modified by constriction, as it is the case in an aqueous environment.

Experimental

Preparation of cylindrical and conically shaped pores. Single pores were prepared in 12 μm thick polyethylene terephthalate (PET) films by the track-etching technique.³³ The irradiation with single energetic heavy ions (Au and U with energy of 11.4 MeV/u) was performed at the linear heavy ion accelerator UNILAC at the GSI Helmholtzzentrum für Schwerionenforschung GmbH in Darmstadt, Germany.³⁴ The films were subsequently exposed to UV radiation at a wavelength of 365 nm for 1 hour per side, followed by wet chemical etching in sodium hydroxide. In order to achieve cylindrical shape of the pore, the etching was performed in 2 M NaOH at 60 °C. The pore opening is known to increase linearly with the etching time, and in our conditions, 30 minutes of etching led to pores with an opening diameter of ~ 400 nm.³⁵ In order to obtain pores of a desired opening, the etching time was adjusted accordingly.

The diameter of single pores was subsequently measured by recording current-voltage curves in 1 M KCl and relating the pore resistance with its geometry. The measurements were performed with the Keithley picoammeter/voltage source. The high concentration of the background electrolyte assured effective screening of charges of the pore wall² so that we can assume that the conductivity of the medium in the pore is equal to the conductivity in the bulk. The pore diameter, d , can be then easily calculated from the formula, which relates the pore resistance with its geometry:

$$R = \frac{4L}{\sigma\pi d^2} \quad (1)$$

where σ is the conductivity of the electrolyte, and L is the thickness of the membrane. Pores with openings between 350 nm and 1 μm in diameter were investigated.

Experiments were also performed with few conically shaped nanopores whose narrow opening was below 100 nm in diameter. The pores were obtained by asymmetric etching in 9 M NaOH as described before.³⁶ The pore opening diameter was calculated from an equation relating the pore resistance, R , with the narrow, d , and the wide opening, D , diameters:

$$R = \frac{4L}{\sigma\pi dD} \quad (2)$$

Ionogel Synthesis and Casting. The ionogel was synthesized as described previously.³² Briefly, equal volumetric amounts of TMOS (tetramethylorthosilicate, Sigma Aldrich), VTEOS (trimethyloxyvinylsilane, Sigma Aldrich), and formic acid (97% Sigma Aldrich) were sonicated until mixed. A 3/3/1 volumetric ratio of the silica precursor solution (TMOS, VTEOS, and formic acid) / ionic liquid electrolyte/cyclohexane was prepared and aged for 4 hours at -20 °C before processing (1.4/1/5.6/2.1/2.1 mole ratio). The ionogel sol (25 μl) was drop cast onto each side of the membrane. Gels were allowed to react for 24 hours to finish the condensation reaction.

To probe ionic conductivity of the ionogels, two types of measurements were performed. Current-voltage curves were recorded with the Keithley picoammeter/voltage source. Voltage was changed with 100 mV steps; the voltage was kept at each voltage for 3 seconds and a current measurement was taken. At least three voltage scans were performed and the ion current values reported are averages performed over all scans. For conically shaped pores, ion current series in time were recorded as well using sampling frequency of 10 kHz, and low-

pass Bessel filter set at 2 kHz (Axopatch 200B, Digidata 1322A, Molecular Devices, Inc).

the FPGA card and monitored in real time with Axon Digidata 1440A (Molecular Devices, Sunnyvale, CA) and Clampex 10.6 (Molecular Devices). The surface charge information was also

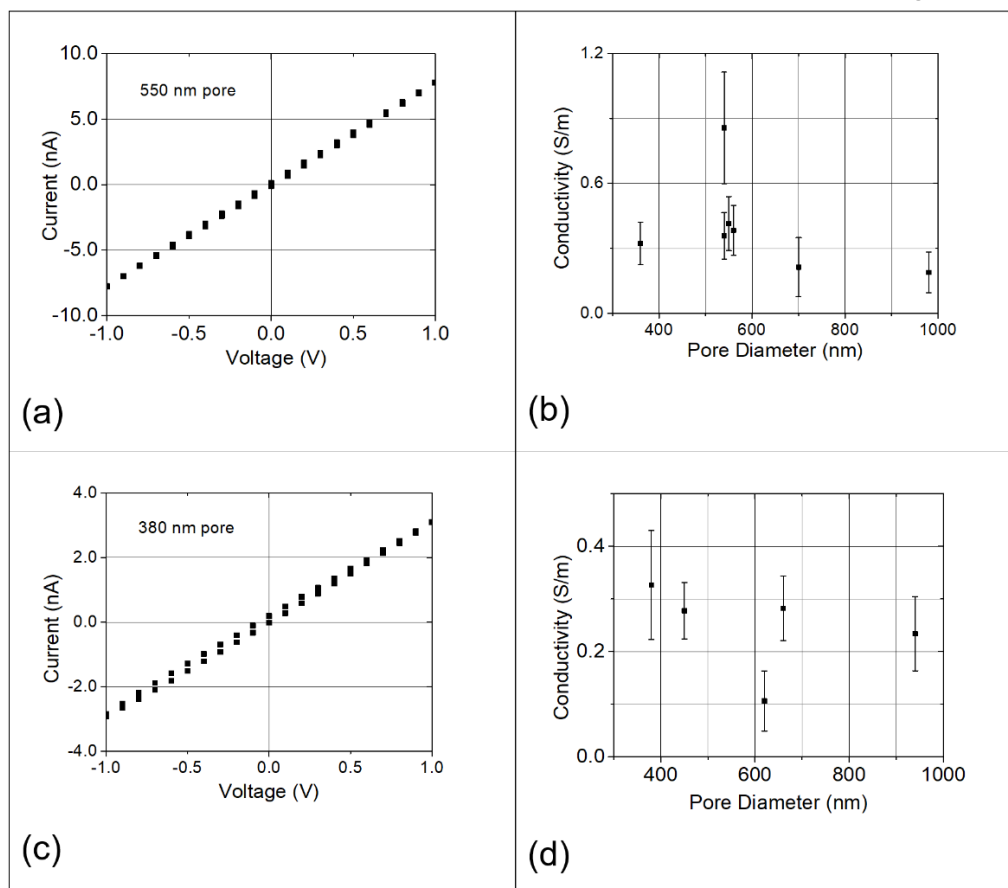


Figure 3. (a) An example current-voltage curve recorded for a 550 nm in diameter pore according to the schematics in Figure 2a together with values of ionic conductivity obtained based on independently measured pores (b). (c) An example current-voltage curve for a 380 nm in diameter pore, and values of ionic conductivity of the ionogel (d) obtained with electric contacts placed directly in contact with ionogel (see the schematics in Figure 2b).

Surface charge mapping protocol. Surface charge mapping was achieved with a home-made Scanning Ion Conductance Microscope (SICM). The setup was the same as described previously.³⁷ Briefly, an electrolyte filled nanopipette was used as the probe, and a Ag/AgCl electrode was back-inserted into the pipette and used as the working electrode (WE). Another Ag/AgCl electrode was placed in the bulk electrolyte and worked as the reference electrode (RE). A constant potential difference was applied between WE and RE to generate an ion current, which was used as a feedback to control the movement of the pipette. For simultaneous surface charge and topography measurement, the SICM feedback loop was controlled with a customized FPGA board (Diligent, Inc., Pullman, WA) and user interface. In the experiment, hopping mode³⁸ was adopted as the scan mode to acquire topographic information. At the beginning (pipette retracted) and end (pipette extended) of each “hop” at each imaging pixel, the feedback loop was paused for a time period, during which the applied potential difference was swept in a preset range, typically, -0.8 V to 0.8 V in 19 even steps. The resultant current at each step was collected through

processed via the FPGA card during scanning. At each pixel, current-voltage response (I-V curve) was plotted when the pipette was retracted and extended. Ion current rectification ratios (ICRRs)³⁹ were calculated for both I-V curves with the following equation:

$$ICRR = \left| \frac{I_{-0.8V}}{I_{0.8V}} \right| \quad (3)$$

where $I_{-0.8V}$ is the current value at -0.8 V and $I_{0.8V}$ is the current value at +0.8 V. The difference between ICRRs was calculated and plotted to generate a surface charge distribution map:

$$ICRR_{difference} = ICRR_{extended} - ICRR_{retracted} \quad (4)$$

where $ICRR_{extended}$ and $ICRR_{retracted}$ represent ion current rectification ratio of the pipette in an extended and retracted position, respectively.

Extended I-V curves on sample surface were calculated by average 100 I-V curves in a selected area (indicated by a white box in images) when the pipette was in an extended position.

The retracted I-V curve was calculated by average all the I-V curves in the scan area.

Results and Discussions

Figure 1 shows a transmission electron microscopy image of the silica matrix of an ionogel, which suggests that when dried, the material contains voids that are on the order of 10 nm in diameter. As shown previously, ionic liquid constitutes at least 80% of the ionogel volume supporting the claim the voids are highly interconnected. It was also demonstrated that ionic liquid containing a lithium salt undergoes destructuring when confined in silica ionogels.⁴⁰ The effect of destructuring causes ion pairs to become destabilized, which enhances conductivity.

In this work we show ionic conductivity of ionogels embedded in single meso- and nanopores. The ability to probe electrochemical properties of confined ionogels is important in the pursuit of creating nano solid-state batteries.³¹ Quantitative characterization of ionogels on meso- and nanoscales would also give insight into inhomogeneities of the ionogel structure.

Ionic conductivity of the ionogel was investigated using two experimental approaches shown in Figure 2. The first set-up is reminiscent of measuring ion current through single nanopores in liquid electrolytes;² a single pore membrane separates two chambers of a conductivity cell filled with the same medium as it is present in the gel. Both sides of the membrane were therefore in contact with ionic liquid BMIM TFSI containing 500 mM Li TFSI. Pellet Ag/AgCl electrodes (A-M Systems, Sequim, WA) were used in the measurements.

Conductivity of the ionogel was also probed without bulk liquid electrolyte present creating an approach that was reminiscent of experiments performed in the solid-state battery set-up. Electrical contacts were provided by sputtering 20 nm of Au on both sides of the membrane after the pore preparation. Drop-casting of the gel was performed in such a way that a large area of Au remained uncovered and available to make electrical connection. The excess of the ionogel on both membrane

surfaces played a role of the ion source. We expected that due to the presence of only one pore in the membrane with an opening diameter below 1 μm , no depletion zone would be formed. The ion current measured is a sum of ion currents carried by all ions present in the solution, thus not only lithium and TFSI but also ions that compose the background ionic liquid.

Figure 3a shows an example current-voltage curve obtained for a pore with an opening diameter of 550 nm studied according to the approach detailed in Figure 2a. A linear character of the recordings allowed us to quantify the pore resistance, which in combination with the pore geometry gave the value of the conductivity of the medium in the pore. Measurements of conductivity for six additional, independently prepared pores are shown in Figure 3b. The error bars were calculated based on the standard deviation of ion current as well as the uncertainty of the pore opening diameter. Note that the average of ionogel conductivity for all pores equals 0.39 S/m, which is in excellent agreement with previous data obtained in the ionogel films.^{40,41}

An example current-voltage curve obtained in the liquid-electrolyte free set-up is shown in Figure 3c alongside with values of ionic conductivity obtained based on 5 pores prepared according to the scheme in Figure 2b. Again an Ohmic behavior was observed in this case, and the conductivity values were similar to these obtained when the liquid electrolyte was present on both sides of the membrane.

The experimental data shown in Figure 3 allowed us to draw the following conclusions. First, the ionic conductivity of the ionogel is not sensitive to the presence of bulk electrolyte, which indicates that ions are most probably sourced from the additional amount of ionogel present on the membrane surface. Second, the ionogel/liquid interface does not contribute to the system resistance. Finally, in the range of pore diameters investigated, between ~ 350 nm and a micron, the ionogel conductivity is not affected by the meso-constriction and the conductivity measured is in agreement with previous bulk studies.

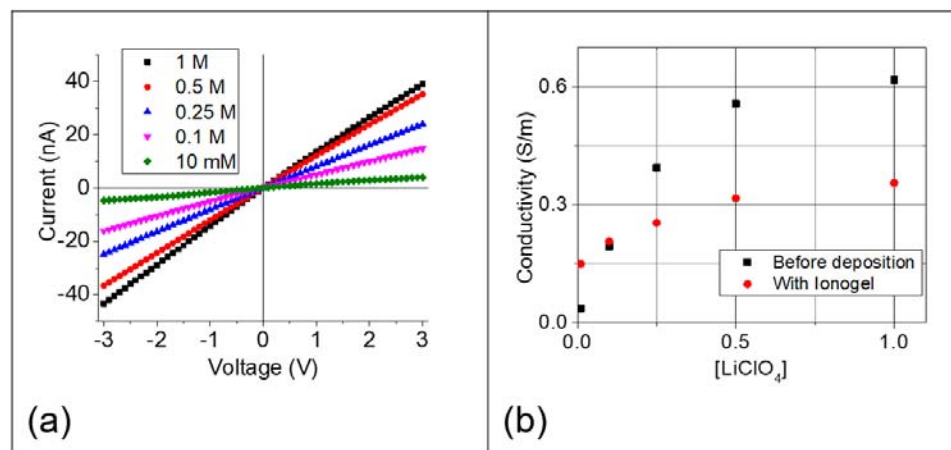


Figure 4. Ion current through a single 730 nm in diameter pore filled with ionogel and placed in contact with propylene carbonate solutions of LiClO_4 . Recordings were performed in symmetric electrolyte conditions on both sides of the membrane with LiClO_4 concentration between 10 mM and 1 M. (b) Conductivity of the ionogel inside the pore as a function of LiClO_4 in the bulk. Data recorded for an empty pore, before gel deposition, is shown as well.

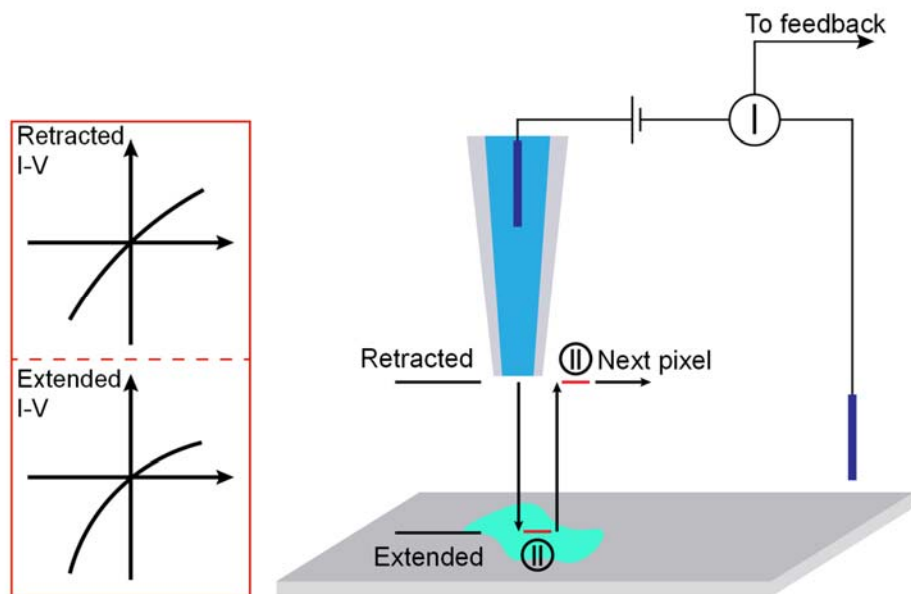


Figure 5. Schematic of the instrument setup for surface charge mapping. Hopping mode was adopted as the scan mode in SICM. At each pixel, the feedback loop was paused temporarily when the pipette reached the control point (extended) and retracted, during which, the applied potential was swept and the resultant current-voltage responses were compared to extract surface charge information.

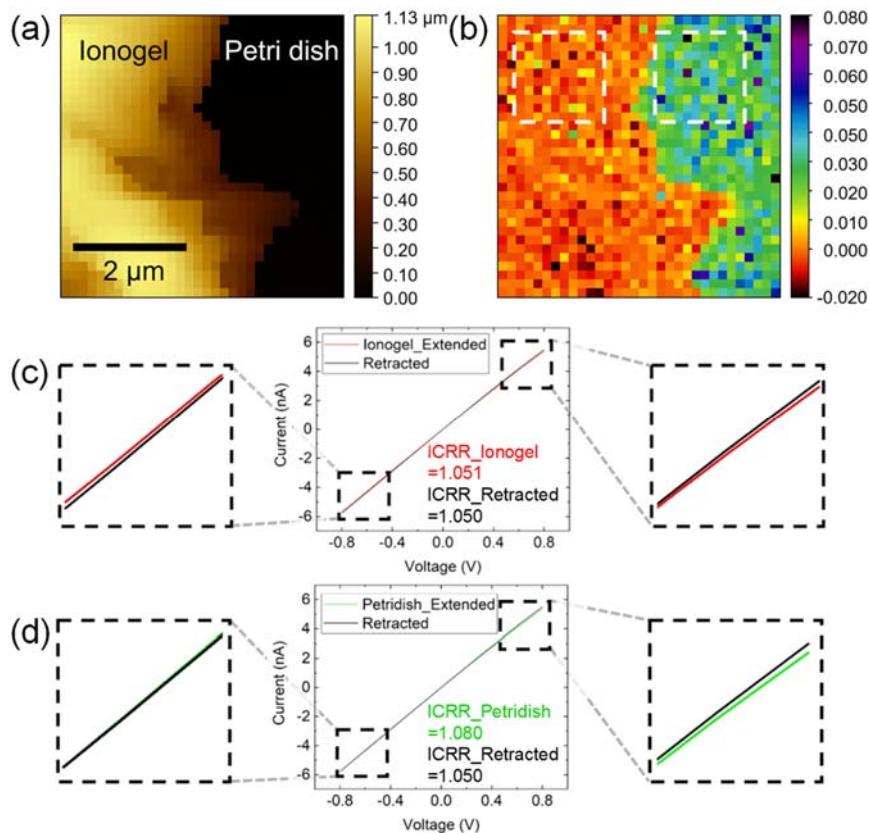


Figure 6. (a) Topography image of an ionogel sample on a petri dish and (b) ICRR difference image of the same area. Extended I-V curves of (c) ionogel surface and (d) petridish surface are plotted together with the retracted I-V curve separately.

The observation of the pore diameter independent conductivity further suggests that the ionogel structure is preserved inside the pores. Previous structural studies revealed that the ionogel contains ~ 10 nm in size interconnected voids (Figure 1),^{32,40,41} which was confirmed in our studies via the finite current through a pore filled with the ionogel.

To provide additional evidence that the voids are interconnected and the ionogel fills the entire volume of the pores we have placed the pores in contact with a solution of propylene carbonate solution of lithium perchlorate. Propylene carbonate is miscible with the ionic liquid, thus propylene carbonate was expected to replace the ionic liquid in the ionogel network. Successful replacement of the electrolyte would be evidenced by the dependence of the measured conductance on the background electrolyte concentration. Figure 4 shows the magnitude of the conductivity calculated based on the pore geometry and resistance obtained from I-V curves. An increase of conductivity with the increase of LiClO_4 concentration in the bulk suggested that indeed ionic concentration in the ionogel is influenced by the bulk electrolyte. The magnitude of conductivity saturated at ~ 500 mM LiClO_4 and reached the magnitude observed with the ionic liquid. Note however that the ionic transport of LiClO_4 in PC is hindered in the ionogel compared to bulk measurements as well as recordings with an as-prepared pore, before ionogel deposition. We believe the lower ionic conductivity of the liquid electrolyte stems from its interactions with the silica surface reported before for the salt.²²

Finally, we asked a question whether the ionogel filled with ionic liquid containing lithium carries net charge. Silica is known to be negatively charged, however in contact with ionic liquid, one could expect the surface charges to be largely screened. Moreover, Li^+ ions were shown to adsorb on surfaces reducing the effective surface charge.⁴² To understand the charge properties of the ionogel, experiments that made use of scanning ion conductance microscopy (SICM) were performed. SICM involves a glass nanopipette filled with electrolyte (100

mM KCl solution, pH was adjusted to 4 with 1M HCl) and a petri dish with deposited gel immersed containing the same electrolyte. We used aqueous electrolyte in the pipette and petri dish, because it allowed us to maximize the current signal and BMIM TFSI is not miscible with water.

Figure 6 shows examples of recorded data showing the topography image, $\text{ICRR}_{\text{difference}}$ (eq. (4)), as well as extended I-V curves on ionogel surface, on petri dish surface, and retracted I-V curve. A clear contrast between the ionogel and petri dish surface was observed and matched well with the topography image (Figure 6a and b). ICRR difference value is close to 0 on ionogel surface while more positive on petri dish, which indicates that surface charge of ionogel is screened in KCl solution. Sample I-V curves on ionogel surface and petri dish surface were plotted by averaging all the I-V curves in the dash line square separately (Figure c and d). Although the difference is not very obvious when comparing with retracted I-V curve (black line in Figure 6 c,d), it can be distinguished with ICRR values, which also supports the claim that the charge of ionogel is screened in solution.

Measurements of ionic conductivity shown above have been performed using meso-structures with opening diameters of few hundreds of nanometers. In order to probe ionic transport in ionogels at the nanoscale we prepared conically shaped nanopores with the tip diameter between 20 nm and 100 nm; the large opening of the cone-shaped pores was ~ 1 μm . An example recording is shown in Figure 7. In this case, we have performed two types of measurements, current-voltage curves as it was done for the cylindrically shaped pores, as well as ion current in time with sampling frequency of 10 kHz. 100 s long recordings were performed at each voltage step between -1V and +1V, which allowed us to conclude the current was stable and the amount of additional ionogel present on membrane surfaces sustained the transport without any signal decay. The current-voltage curves were nearly linear, which is in agreement with the finding of nearly no effective surface charge of the ionogel in contact the ionic liquid. Based on the I-V curve we estimated the conductivity to be ~ 0.4 S/m.

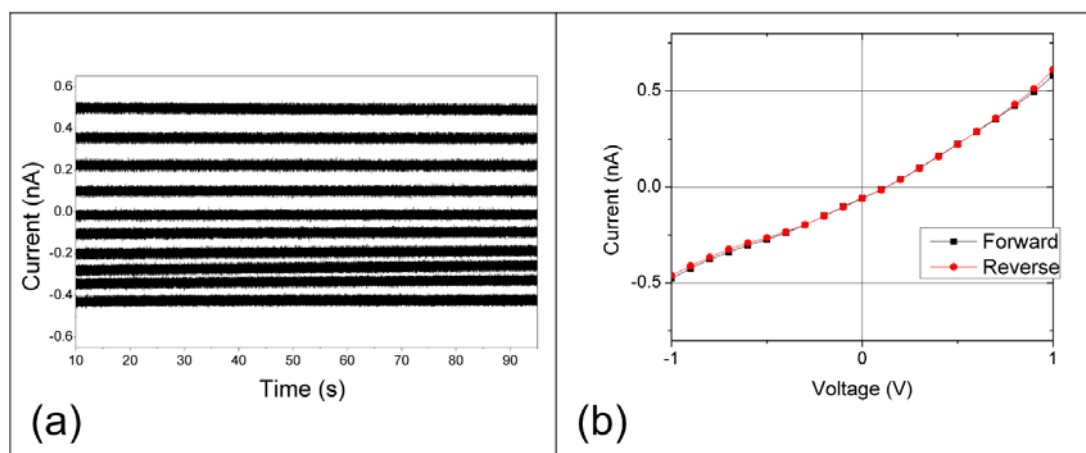


Figure 7. Ion current through a single conical nanopore with opening diameters of 20 nm (tip) and 1 μm (base) filled with the silica ionogel. (a) Ion current signals in time recorded between -1V and +1V with 100 mV voltage step. Recordings for -1V, -0.8V, -0.6 V ...+1V are shown. (b) Current-voltage curve recorded from the time signals for forward and reverse scans. The small current at 0V is caused by the instrument offset.

Conclusions

In this manuscript we proposed a method to probe ionic transport properties of solid electrolytes at the nano- and meso-scales. We proposed two experimental approaches to quantify ionic conductivity. The first method involves a liquid electrolyte and the experimental set-up is similar to what has been known in experiments with liquid electrolytes. The second approach requires placing electrical contacts on the membrane and ion current can be probed without any reservoirs with liquid. Applicability of the methods proposed was demonstrated for an ionogel based electrolyte, however the same concept can be used to investigate ionic conductivity of any solid electrolyte.

In the next step, we will prepare pores with much smaller opening diameter to investigate at which size the conductivity will be influenced by the nano-confinement.

Conflicts of interest

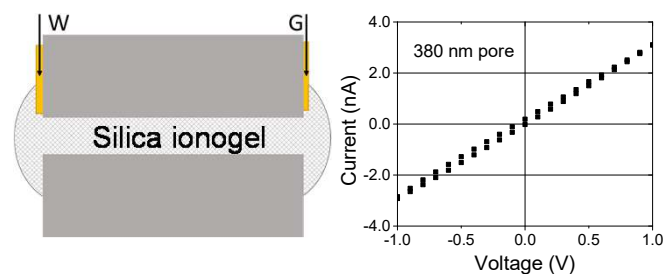
Acknowledgements

ZS acknowledges the Nanostructures for Electrical Energy Storage (NEES), an Energy Frontier Research Center funded by the US Department of Energy, Office of Science, Office of Basic Energy Sciences under Award Number DESC001160. We also acknowledge GSI Helmholtzzentrum für Schwerionenforschung in Darmstadt, Germany for providing irradiated membranes as well as Dr. Phillip Collins for valuable conversations during the course of the research. LAB and CZ acknowledge the National Science Foundation and CMI award 1507341 for support of this work.

Reference

- B. Hille, *Ion Channels of Excitable Membranes*; Sinauer Associates: Sunderland, MA, 2001.
- R.B. Schoch, J. Han and P. Renaud, Transport Phenomena in Nanofluidics, *Rev. Mod. Phys.*, 2008, **80**, 839-883.
- I. Vlassiok, S. Smirnov and Z.S. Siwy, Ion Selectivity of Single Nanochannels, *Nano Lett.*, 2008, **8**, 1978-1985.
- C. Wei, A. J. Bard and S. W. Feldberg, Current Rectification at Quartz Nanopipet Electrodes, *Anal. Chem.*, 1997, **69**, 4627-4633.
- Z. Siwy and A. Fulinski, Fabrication of a Synthetic Nanopore Ion Pump, *Phys. Rev. Lett.*, 2002, **89**, 198103.
- Z. S. Siwy, Ion Current Rectification in Nanopores and Nanotubes with Broken Symmetry Revisited, *Adv. Funct. Mater.*, 2006, **16**, 735-746.
- J. Cervera, B. Schiedt and P. Ramirez, A Poisson/Nernst-Planck Model for Ionic Transport through Synthetic Conical Nanopores, *Europhys. Lett.*, 2005, **71**, 35-41.
- M. Ali, P. Ramirez, S. Mafé, R. Neumann and W. Ensinger, A pH-Tunable Nanofluidic Diode with a Broad Range of Rectifying Properties, *ACS Nano*, 2009, **3**, 603-608.
- G. Perez-Mitta, A.G. Albesa, C. Trautmann, M.E. Tomil-Molares and O. Azzaroni, Bioinspired Integrated Nanosystems Based on Solid-State Nanopores: "Iontronic" Transduction of Biological, Chemical and Physical Stimuli, *Chem. Sci.*, 2017, **8**, 890-913.
- H.S. White and A. Bund, Ion Current Rectification at Nanopores in Glass Membranes, *Langmuir*, 2008, **24**, 2212-2218.
- H. Zhang, Y. Tian and L. Jiang, Fundamental Studies and Practical Applications of Bioinspired Smart Solid-State Nanopores and Nanochannels, *Nano Today*, 2016, **11**, 61-81.
- N. Laohakunakorn and U.F. Keyser, Electroosmotic Flow Rectification in Conical Nanopores, *Nanotechnol.* 2015, **26**, 275202.
- P. Jin, H. Mukaibo, L.P. Horne, G.W. Bishop and C.R. Martin, Electroosmotic Flow Rectification in Pyramidal-Pore Mica Membranes, *J. Am. Chem. Soc.* 2010, **132**, 2118-2119.
- Z. Siwy, L. Trofin, P. Kohli, L.A. Baker, C. Trautmann and C.R. Martin, Protein Biosensors Based on Functionalized Conical Gold Nanotubes, *J. Am. Chem. Soc.*, 2005, **127**, 5000-5001.
- Z.S. Howorka and Z.S. Siwy, Nanopore Analytics: Sensing of Single Molecules, *Chem. Soc. Rev.* 2009, **38**, 2360-2384.
- M. Wanunu, Nanopores: A Journey Towards DNA Sequencing, *Phys. Life Rev.* 2012, **9**, 125-158.
- Y. Tian, L. Wen, X. Hou, G. Hou and L. Jiang, Bioinspired Ion-Transport Properties of Solid-State Single Nanochannels and Their Applications in Sensing, *Chem. Phys. Chem.*, 2012, **13**, 2455-2470.
- W. Shi, A.K. Friedman and L.A. Baker, Nanopore Sensing, *Anal. Chem.* 2017, **89**, 157-188.
- M. Davenport, A. Rodriguez, K.J. Shea and Z.S. Siwy, Squeezing Ionic Liquids through Nanopores, *Nano Lett.*, 2009, **9**, 2125-2128.
- C. Tasserit, A. Koutsioubas, D. Lairez, G. Zalcer and M.-C. Clochard, Pink Noise of Ionic Conductance through Single Artificial Nanopores Revisited, *Phys. Rev. Lett.*, 2010, **105**, 260602.
- X. Yin, S. Zhang, Y. Dong, S. Liu, J. Gu, Y. Chen, X. Zhang, X. Zhang and Y. Shao, Ionic current rectification in organic solutions with quartz nanopipettes, *Anal. Chem.*, 2015, **87**, 9070-9077.
- T. Plett, W. Shi, Y. Zeng, W. Mann, I. Vlassiok, L.A. Baker and Z.S. Siwy, Rectification of Nanopores in Aprotic Solvents - Transport Properties of Nanopores with Surface Dipoles, *Nanoscale*, 2015, **7**, 19080-19091.
- H.B. Park, J. Kamcev, L.M. Robeson, M. Elimelech and B.D. Freeman, Maximizing the Right Stuff: The Trade-Off between Membrane Permeability and Selectivity, *Science*, 2017, **356**, eaab0530.
- L. Xia, L. Yu, D. Hu and G.Z. Chen, Electrolytes for Electrochemical Energy Storage, *Mater. Chem. Front.*, 2017, **1**, 584-618.
- A.M. Stephan, Review on gel polymer electrolytes for lithium batteries, *Eur. Polym. J.* 2006, **42**, 21-42.
- W. Li, Y. Pang, J. Liu, G. Liu, Y. Wang and Y. Xia, A PEO-Based Gel Polymer Electrolyte for Lithium Ion Batteries, *RSC Adv.*, 2017, **7**, 23494.
- M.L. Thai, G.T. Chandran, R.K. Dutta, X. Li and R.M. Penner, 100k Cycles and Beyond: Extraordinary Cycle Stability for MnO₂ Nanowires Imparted by a Gel Electrolyte, *ACS Energy Lett.*, 2016, **1**, 57-63.
- K. Kerman, A. Luntz, V. Viswanathan, Y.M. Chiang and Z. Chen, Review—Practical Challenges Hindering the Development of Solid State Li Ion Batteries. *J. Electrochem. Soc.*, 2017, **164**, A1731-A1744.
- T.S. Plett, W. Cai, M.L. Thai, I.V. Vlassiok, R.M. Penner and Z.S. Siwy, Solid-State Ionic Diodes Demonstrated in Conical Nanopores, *J. Phys. Chem. C*, 2017, **121**, 6170-6176.
- T.W. Plett, M.L. Thai, J. Cai, I. Vlassiok, R.M. Penner and Z.S. Siwy, Ion Transport in Gel and Gel-Liquid Systems for LiClO₄-doped PMMA at the Meso- and Nanoscales, *Nanoscale*, 2017, **9**, 16232-16243.
- A.J. Pearce, T.E. Schmitt, E.J. Fuller, F. Elgabaly, C. Lin, K. Gerasopoulos, A.C. Kozen, A.A. Talin, G. Rubloff, G., and K.E. Gregorczyk, Nanoscale Solid State Batteries Enabled by Thermal Atomic Layer Deposition of a Lithium

- Polyphosphazene Solid State Electrolyte, *Chem. Mater.*, 2017, **29**, 3740–3753.
- 32 D.S. Ashby, R.H. DeBlock, C.H. Lai, C.S. Choi and B.S. Dunn, Patternable, Solution-Processed Ionogels for Thin-Film Lithium-Ion Electrolytes, *Joule* 2017, **1**, 1-15.
- 33 R.L. Fleischer, P.B. Price and R.M. Walker, *Nuclear Tracks in Solids: Principles and Applications*; University of California Press: Berkeley CA; 1975.
- 34 R. Spohr, Methods and Device to Generate a Predetermined Number of Ion Tracks, German Patent, DE2951376C2, 1983; US Patent 4369370, 1983
- 35 S. Müller, C. Schötz, O. Picht, W. Sigle, P. Kopold, M. Rauber, I. Alber, R. Neumann and M.E. Toimil-Molares, Electrochemical Synthesis of $\text{Bi}_{1-x}\text{Sb}_x$ Nanowires with Simultaneous Control on Size, Composition, and Surface Roughness, *Cryst. Growth Des.*, 2012, **12**, 615-621.
- 36 P. Y. Apel, Y. E. Korchev, Z. Siwy, R. Spohr and M. Yoshida, Diode-like single ion-track membrane prepared by electro-stopping, *Nucl. Instrum. Methods in Physics Research, Section B*, 2001, **184**, 337-346.
- 37 L. Zhou, Y. Gong, J. Hou and L.A. Baker, Quantitative Visualization of Nanoscale Ion Transport, *Anal. Chem.*, 2017, **89**, 13603-13609.
- 38 P. Novak et al., Nanoscale Live-Cell Imaging Using Hopping Probe Ion Conductance Microscopy, *Nature Methods*, 2009, **6**, 279-281.
- 39 N. Sa and L.A. Baker, Rectification of Nanopores at Surfaces, *J. Am. Chem. Soc.* 2011, **133**, 10398-10401..
- 40 A. Guyomard-Lack, P.-E. Delannoy, N. Dupre, C.V. Cerclier, B. Humbert and J. Le Bideau, Deconstructing ionic liquids in ionogels: enhanced fragility for solid devices, *Phys. Chem. Chem. Phys.*, 2014, **16**, 23639–23645.
- 41 S.A.M. Noor, P.M. Bayley, M. Forsyth and D.R. MacFarlane, Ionogels based on ionic liquids as potential highly conductive solid state electrolytes. *Electrochim. Acta*, 2013, **91**, 219–226
- 42 T. Gamble, K. Decker, T.S. Plett, M. Pevarnik, J.F. Pietschmann, I. Vlassiuk, A. Aksimentiev and Z.S. Siwy, Rectification of ion current in nanopores depends on the type of monovalent cations: Experiments and Modeling, *J. Phys. Chem. C* 2014, **118**, 9809-9819.



Ionic conductivity of silica ionogel based solid electrolyte on meso and nanoscales is measured.